

# Accepted manuscript doi: 10.1680/jgein.20.00027

---

## **Accepted manuscript**

As a service to our authors and readers, we are putting peer-reviewed accepted manuscripts (AM) online, in the Ahead of Print section of each journal web page, shortly after acceptance.

## **Disclaimer**

The AM is yet to be copyedited and formatted in journal house style but can still be read and referenced by quoting its unique reference number, the digital object identifier (DOI). Once the AM has been typeset, an 'uncorrected proof' PDF will replace the 'accepted manuscript' PDF. These formatted articles may still be corrected by the authors. During the Production process, errors may be discovered which could affect the content, and all legal disclaimers that apply to the journal relate to these versions also.

## **Version of record**

The final edited article will be published in PDF and HTML and will contain all author corrections and is considered the version of record. Authors wishing to reference an article published Ahead of Print should quote its DOI. When an issue becomes available, queuing Ahead of Print articles will move to that issue's Table of Contents. When the article is published in a journal issue, the full reference should be cited in addition to the DOI.

# Accepted manuscript doi: 10.1680/jgein.20.00027

---

**Submitted:** 14 January 2020

**Published online in 'accepted manuscript' format:** 01 May 2020

**Manuscript title:** Predicting strength of soilbags under cyclic compression

**Authors:** F. Jia<sup>1</sup>, S.-H. Liu<sup>2</sup>, C.-M. Shen<sup>1</sup> and Y. Sun<sup>1</sup>

**Affiliations:** <sup>1</sup>College of Water Conservancy and Hydropower Engineering, Hohai University, Nanjing, China and <sup>2</sup>State Key Laboratory of Hydrology-Water Resources and Hydraulic Engineering, College of Water Conservancy and Hydropower Engineering, Hohai University, Nanjing, China

**Corresponding author:** S.-H. Liu, State Key Laboratory of Hydrology-Water Resources and Hydraulic Engineering, College of Water Conservancy and Hydropower Engineering, Hohai University, Xi-Kang Road #1, Nanjing 210098, China.

**E-mail:** [sihongliu@hhu.edu.cn](mailto:sihongliu@hhu.edu.cn)

**Abstract**

Soilbags have a wide range of applications in geotechnical engineering. To explore the compressive strength and deformation behaviour of soilbags, a formula for predicting the strength of soilbags is derived considering the relationship between the tensile force of the bag and the vertical strain. A soilbag under cyclic compression is numerically simulated using the discrete element method to verify the basic stress formula and the derived formula for the tensile force. The results indicate that the increase and distribution of the tensile force in the bag material have an important effect on the compressive strength of soilbags. The derived formula can predict the compressive strength of soilbags under vertical loading, providing a theoretical basis and design methods for structures built with soilbags.

**Keywords:** Geosynthetics, Soilbags, Strength formula, Discrete element method (DEM), Cyclic compression

## 1 INTRODUCTION

Soilbags are woven geotextile bags filled with granular materials such as clays, sands, or crushed stones. They have a wide range of applications in geotechnical engineering (Matsuoka and Liu 2006, 2007; Wang et al. 2015; Liu et al. 2015, 2017, 2019, 2020; Fan et al. 2019; Wang et al. 2019a, 2019c; Sheng et al. 2020). According to Matsuoka et al. (1999, 2003), soilbags have a high strength when subjected to an external load. This feature is primarily attributed to the mobilization of tensile forces in the bags. Other advantages of soilbags that make them suitable as foundations and embankment materials are their low vibration (Liu et al. 2014; Ding et al. 2018), resistance to frost heave (Li et al. 2013), and low environmental impact (Matsuoka and Liu 2006; Liu 2017). To ensure the stability and safety of soilbag-built structures, the cyclic compressive strength and deformation behaviour of soilbags must be considered (Pham et al. 2020).

As a new type of reinforced soil structure, the strength and deformation characteristics of soilbags have been simulated by different numerical methods (Tantono and Bauer 2008a; Ye et al. 2011; Cheng and Yamamoto 2015). The mechanical behaviour of a soilbag under increasing vertical compression was numerically simulated by Tantono and Bauer (2008b) using a micro-polar continuum approach. Ansari et al. (2011) presented a finite element model for analysing the behaviour of granular material wrapped in polyethylene bags under vertical compression and validated the effectiveness of soilbags as a method of ground improvement. Cheng et al. (2016b, 2017) numerically investigated the stress states and geotextile anisotropies of wrapped soil under unconfined compression using the discrete element method (DEM). To investigate the compressive strength and deformation behaviour of soilbags, various theoretical studies analysed the compressive strength of soilbags. On the basis of the limit equilibrium condition of the soil, the limit strength formula for soilbags in 2D space has been obtained (Matsuoka et al. 2003). Using the generalized Mises failure criterion and the Lade–Duncan failure criterion, two ultimate compressive strength formulas have been derived for soilbags under complicated stress conditions in 3D space (Bai et al. 2010). Liu et al. (2018) developed a 2D strength formula for soilbags under inclined loads and verified it through DEM simulations. In these formulas, the tensile force of the bag  $T$  is often regarded as a constant or is fitted from numerical simulation results, but this is either unrealistic or impractical. Thus, the abovementioned strength formulas are not applicable to soilbags during the loading/unloading compressive process, because they ignore the relationship between the tensile force  $T$  and the vertical strain (Liu 2016). Thus, this paper describes the derivation of a quantitative relationship between the tensile force in the bag

and the vertical strain on the soilbag, and verifies the resulting formula through DEM simulations of a laboratory test.

## 2 STRENGTH FORMULA FOR SOILBAGS CONSIDERING VERTICAL STRAIN

Fig. 1(a) shows a soilbag subjected to the external principal stresses  $\sigma_1$  and  $\sigma_3$  in a 2D manner (Matsuoka and Liu 2003). Under the action of vertical loading, the soilbag tends to be flat. According to the reverse isoperimetric inequality (Ball 1991), the flattened bag will be elongated, which induces a tensile force along the bag and produces an additional stress acting on the wrapped soil, as shown in Fig. 1(b).

Thus, the stress of the soil wrapped in the bag  $\sigma_s$  is the sum of the externally applied stress  $\sigma$  and the additional stress produced by the tension of the bag  $\sigma_T$ :

$$\sigma_s = \sigma + \sigma_T \quad (1)$$

The matrix form of the externally applied stress  $\sigma$  in the xy space can be written as:

$$\sigma = \begin{bmatrix} \sigma_3 & 0 \\ 0 & \sigma_1 \end{bmatrix} \quad (2)$$

and the matrix form of the additional stress produced by the tension of the bag  $\sigma_T$  is:

$$\sigma_T = \begin{bmatrix} \frac{2T}{H} & 0 \\ 0 & \frac{2T}{B} \end{bmatrix} \quad (3)$$

By substituting Eqs. (2) and (3) into Eq. (1), the stress of the soil wrapped in the bag  $\sigma_s$  can be obtained:

$$\sigma_s = \begin{pmatrix} \sigma_3 + \frac{2T}{H} & 0 \\ 0 & \sigma_1 + \frac{2T}{B} \end{pmatrix} \quad (4)$$

It is assumed that the failure of soilbags is accompanied by the shear failure of the wrapped soil, which is governed by the Mohr–Coulomb failure criterion. This assumption is expressed in terms of the major and minor principal stresses as:

$$\frac{\sigma_{1s} - \sigma_{3s}}{2} = \frac{\sigma_{1s} + \sigma_{3s}}{2} \sin \varphi_s + c_s \cos \varphi_s \quad (5)$$

where  $\sigma_{1s}$ ,  $\sigma_{3s}$  are the major and minor principal stresses of the wrapped soil, respectively and  $c_s$ ,  $\varphi_s$  are the cohesion and the internal friction angle of the wrapped soil, respectively.

$\sigma_{1s}$  and  $\sigma_{3s}$  can be calculated from the eigenvalues of the stress tensor  $\boldsymbol{\sigma}_s$  in Eq. (4). Substituting these quantities into Eq. (5) yields:

$$\frac{\sigma_1 - \sigma_3}{2} = \frac{\sigma_1 + \sigma_3}{2} \sin \varphi_s + \left( \frac{T}{H} - \frac{T}{B} \right) + \left( \frac{T}{H} + \frac{T}{B} \right) \sin \varphi_s + c_s \cos \varphi_s \quad (6)$$

By comparing Eq. (5) with Eq. (6), the relationship between  $\sigma_1$  and  $\sigma_3$  expressed in Eq. (6) can be regarded as having the same form as the Mohr–Coulomb equation, implying that the soilbag has the same failure mode as the wrapped soils. Thus, the additional cohesion  $c_T$  of the soilbag produced by the tensile force  $T$  can be obtained from Eq. (6) as:

$$c_T = \left( \frac{T}{H} - \frac{T}{B} \right) \frac{1}{\cos \varphi_s} + \left( \frac{T}{H} + \frac{T}{B} \right) \tan \varphi_s \quad (7)$$

Fig. 2 shows a snapshot of a single bag before and after compression. The bag consists of line section AB and arc section BC (semicircle). The length of line section AB is  $l$ , the radius of arc section BC is  $r$ , and the vertical strain on the bag body is  $\varepsilon$ .

The relationship between the tensile force and the vertical strain can be derived on the basis of the following two assumptions: (1) The volume of the wrapped soil (that is, the area in two dimensions) remains constant; (2) The shape of the soilbag always consists of two semicircles and two straight lines.

According to the above conditions, the formula for calculating the total length of the bag and the area of the soilbag before/after compression can be obtained.

$$L_0 = 2\pi r_0 + 2l_0 \quad (8)$$

$$S_0 = \pi r_0^2 + 2r_0 l_0 \quad (9)$$

$$L_1 = 2\pi(1 - \varepsilon)r_0 + 2l_1 \quad (10)$$

$$S_1 = \pi(1 - \varepsilon)^2 r_0^2 + 2(1 - \varepsilon)r_0 l_1 \quad (11)$$

Based on assumption 1, the volume of the wrapped soil remains constant, that is:

$$S_1 = S_0 \quad (12)$$

By substituting Eqs. (9) and (11) into Eq. (12), one can obtain the length of the line section after compression:

$$l_1 = \frac{\pi r_0 \varepsilon (2 - \varepsilon) + 2l_0}{2(1 - \varepsilon)} \quad (13)$$

Combining Eqs. (8), (10), and (13), the relationship between the change in bag length and the vertical strain on the soilbag can be expressed as follows:

$$\Delta L = \frac{\pi \varepsilon^2 r_0 + 2\varepsilon l_0}{1 - \varepsilon} \quad (14)$$

According to Eq. (14), if the volume of the wrapped soil remains constant, the total length of the bag varies with the deformation of the wrapped soil. As the woven bag is a linear elastic material, the tensile force of the bag can be described by the variation in the length of the bag:

$$T = k\Delta L \quad (15)$$

By substituting Eqs. (14) and (15) into Eq. (7), the apparent cohesion  $c_T$  of the soilbags produced by the tensile force  $T$  can be described as follows:

$$c_T = k \frac{\pi \varepsilon^2 r_0 + 2\varepsilon l_0}{1 - \varepsilon} \left[ \left( \frac{1}{H} - \frac{1}{B} \right) \frac{1}{\cos \varphi_s} + \left( \frac{1}{H} + \frac{1}{B} \right) \tan \varphi_s \right] \quad (16)$$

### 3 DEM ANALYSIS OF A SOILBAG UNDER VERTICAL CYCLIC LOADING

#### 3.1 Outline of the DEM analysis

In section 2, the strength formula for soilbags under vertical loading was derived based on the Mohr–Coulomb failure criterion. Next, the results of uniaxial compression tests on a soilbag will be numerically analysed using DEM to verify the derived formula for the strength of soilbags.

DEM is a numerical method that was pioneered by Cundall (1971) for computing the motion and effect of a large number of small particles, and was later applied to soils by Cundall and Strack (1979). With advances in computing power and numerical algorithms for nearest-neighbour sorting, it is possible to numerically simulate millions of particles on a single processor. Today, DEM is widely accepted as an effective means of addressing engineering problems in granular and discontinuous materials, especially in granular flows, powder mechanics, and rock mechanics.

In two dimensions, each particle has three degrees of freedom (two translations and one rotation). Each particle can be in contact with neighbouring particles or structure boundaries. The contact between two particles, or between a particle and a boundary, is modelled by a spring and dashpot in both the normal and tangential directions. The normal direction spring has a no-tension constraint. In the tangential direction, if the tangential force reaches the Coulomb friction limit, it is allowed to slide. Small amounts of viscous damping are often included to provide dissipation of high-frequency motion. The forces generated during contact are computed based on the overlap of the bodies at the contact point and the stiffness of the springs, and these forces are then used to compute the acceleration of the body according to Newton's laws of motion. After the acceleration has been determined, the new velocity and displacement values for the particle are computed using central-difference explicit-time integration. With the newly computed displacement configuration, the state of deformation at the existing contacts is re-evaluated and the possible creation of new contacts is evaluated, leading to a new cycle of computation. In this study, the numerical simulations are conducted using the commercial PFC<sup>2D</sup> (Particle Flow Code in 2D) software. The time increment  $\Delta t$  is computed automatically by PFC<sup>2D</sup>, and is no more than  $5 \times 10^{-6}$  s.

### **3.2 Modelling a flexible bag**

In conventional contact models, forces between particles are only generated when they are in contact. The normal-direction spring has a no-tension constraint. Obviously, this model is not suitable for a flexible bag that can only withstand tension but not compression. In this study, the flexible bag is modelled as a series of mono-sized circular particles connected by a parallel bond. The parallel bond in this study is a linear-based model installed at two neighbouring bag particles (Lu and McDowell 2010). The tensile force generated when the distance between two neighbouring bag particles is elongated is computed based on the elongated distance and the stiffness of the spring. The parallel bond strength corresponds to the tensile strength of the woven bag in the elastic range, as determined by a tensile test.

### **3.3 Simulation of uniaxial compression tests**

Firstly, a DEM model of one soilbag with a width  $B = 40$  cm and a height  $H = 10$  cm is generated. The model consists of two semicircles and one rectangle. The model of the wrapped soil is constructed from 479 circular particles with random diameters ranging from 4–16 mm. The particles in the DEM model are randomly generated within the bag boundary, and they may overlap with each other. The radius of the soil particles is reduced and then expanded several times until reaching the required size. To dissipate the disturbances caused

by the radius expansion, a number of DEM calculation cycles are performed until the force ratio (the ratio of the average sum of the contact force and body force magnitudes to the total sum of the applied force and body force magnitudes over all bodies) is less than  $10^{-5}$ . The prepared sample is basically isotropic and the difference between the geotextile components in the x and y directions is less than 5%. The bag model is made up of 180 mono-sized bag particles with a diameter of 5 mm. The DEM specimen is bounded by two horizontal rigid walls, as shown in Fig. 3.

The contact between soil particles is modelled using a linear model. The input parameters used in the DEM simulation are summarized in Table 1, and were determined using an assembly of aluminium rods. The aluminium rods are good materials for simulating soil particles in 2D conditions, and these parameters were used to simulate biaxial compression, simple shear, and direct shear tests on an assembly of aluminium rods. The simulated results agree very well with previous experimental results (Yamamoto 1995; Liu and Matsuoka 2003). The contact between bag particles is modelled by a linear parallel bond model. The parameters of the bag model used in DEM are those of the geotextile bag tested by Cheng et al. (2016b) and Wang et al. (2019b). To magnify the deformation effect, the tensile stiffness of the bag in the normal direction is reduced by a reasonable amount. A global non-viscous damping coefficient of 0.3 is chosen to reduce the fluctuations of the response and the gravitational field is neglected to maintain symmetry in the simulations.

The numerical uniaxial compression test on a soilbag is controlled by a servomechanism in the PFC<sup>2D</sup> software. The wall servo provides the ability to control the translational velocity of selected walls using a servomechanism to apply or maintain the desired force. The DEM specimen is preloaded with 2 kPa (vertical force of 0.8 kN) by lowering the top wall before loading. Three cycles of vertical loading are then numerically simulated, as shown in Fig. 4. The vertical force is gradually increased to 24 kN and then decreased to 0.8 kN in each cycle.

### 3.4 Results and discussion

Figs. 5 and 6 show snapshots at different values of vertical stress under the loading and unloading states. The bag particles are coloured blue and the wrapped soil particles are coloured brown. Fig. 5 also shows the evolution of force chains. The contact forces are represented by straight lines connecting the centres of two contacting balls. The magnitude of the contact forces is proportional to the thickness and colour of the force chains. Fig. 6 also shows the vector distribution of the displacement of the wrapped particles. Under a loading of 10 kPa, the contact force between the soil particles in the soilbag is uniformly distributed, and the tensile force is

uniform along the circumference, as shown in Fig. 5(a). As the vertical load increases, the number of particle contact points increases, and the particle contact forces gradually increase. During the loading process, the strong force chains are arranged anisotropically and mainly extend vertically, and the particle contact forces of the central region are much larger than those of the two sides. During the unloading process, the particle contact forces in the soilbag gradually decrease, and the force chain distribution becomes more uniform and isotropic. The vertical strain of the soilbag is quite different before and after cyclic loading due to the plastic deformation of the soilbag during the first loading process.

In the case of  $l_0 = 0.3\text{m}$ ,  $r_0 = 0.05\text{m}$ , the relationship between the change in bag tension and the vertical strain can be calculated using Eqs. (14) and (15). Fig. 7 shows the predicted and simulated evolution of the tensile force  $T$  of the bag during uniaxial compression, where the tensile force is taken as the average of the tensile forces around the circumference of the bag. During the compression process, the tensile force of the bag increases almost linearly with the increase in vertical strain when the vertical strain is small, but this becomes significantly nonlinear when the strain is large. Thus, the tensile force cannot be regarded as a constant or a linear relationship with respect to the vertical strain under large deformation conditions. The predicted change in tensile strength with respect to the vertical strain of the soilbag is larger than given by the numerical simulations, because the volume of the bag is not strictly constant during compression.

Three measurement domains are predetermined (positioned in the middle and two sides of the soilbag) to monitor the stress state of the wrapped soil, as shown in Fig. 3. The average stress tensor of the soil in the three measurement domains is calculated from the interparticle forces (Zhao et al. 2018; Cheng et al. 2019; Shen et al. 2019):

$$\boldsymbol{\sigma}_s = \frac{1}{V} \sum_{n_c} \mathbf{d}^c \otimes \mathbf{f}^c \quad (17)$$

where  $V$  is the volume (area in two dimensions) of the measurement region and  $\mathbf{d}^c$ ,  $\mathbf{f}^c$  are the corresponding branch vector and force vector, respectively, of the contacts.

The stresses on the wrapped soil in the  $y$  direction  $\sigma_{yy}$  and  $x$  direction  $\sigma_{xx}$  during cyclic loading are plotted in Fig. 8. The solid lines in Fig. 8 indicate the stresses of the measurement domains (measured values) computed by Eq. (17). In addition, the stresses on the wrapped soil can be calculated via Eq. (4) using the stress applied on the rigid boundaries and the tensile force from the DEM simulation. This shows that the calculated stresses on

the wrapped soil are basically in agreement with the numerically simulated values, indicating that the basic stress formula of the soilbag is reasonable. Note that the measured stresses are slightly smaller than the calculated ones in the y direction, but slightly larger in the x direction. This is a result of the non-uniform distribution of the tensile force between bag particles in the case of large deformation, as shown in Fig. 5(b). The tensile forces between bag particles on the upper and lower parts of the soilbag are slightly larger than those on the left and right sides.

Fig. 9 shows the cyclic vertical stress versus the vertical strain of the soilbag under vertical cyclic loading. It is obvious that the cyclic compressive stress–strain relation of the soilbag is strongly nonlinear, and obviously different in the loading and unloading states. For a full loading–unloading cycle, the curve forms a closed hysteresis loop. This observation verifies the effectiveness of soilbags in reducing mechanical vibration, as described by Liu et al. (2014).

Cyclic uniaxial compression tests of a 2D soilbag were conducted on a triaxial apparatus without a pressure chamber, as shown in Fig. 10. The wrapped soil was physically modelled by an assembly of 50-mm-long aluminium rods with diameters of 1.6 mm and 3 mm at a ratio of 3:2 by weight, as used in a series of geotechnical experiments (Matsuoka and Liu 2003; Lee and Song 2010). The experimental results of the compression behaviour of soilbags under vertical cyclic loading is shown in Fig. 11. It is clear that the loading–unloading curve forms a closed hysteresis loop, but its shape is slightly different from that of the simulation results in Fig. 9. The stiffness of the soilbag obtained from the experimental loop increases with the number of cyclic compressions, probably a result of the friction in the loading plate during the experiment. To clarify this reason, cyclic compressive simulations were also conducted with a trial calculated plate–bag friction coefficient of 0.2. Fig. 12 presents the simulated stress–strain hysteresis loops, which are similar to the experimental ones. Therefore, the friction between the loading plate and the bag has an effect on the compressive stress–strain relationship of soilbags.

#### **4 CONCLUSIONS**

In this study, the strength characteristics of soilbags under cyclic compression have been investigated. The relationship between the tensile force of the bag and the vertical strain of the soilbag was discussed, and a strength formula for soilbags considering the relationship between the tensile force of the bag and the vertical strain was derived. DEM simulations of a soilbag under vertical cyclic loading were conducted to verify the derived soilbag strength formula. The main results are as follows:

(1) The increase and distribution of the tensile force in the bag material have a major impact on the compressive strength of soilbags. The quantitative relationship between the bag tensile force and the vertical strain on the soilbag can be approximatively described by the deduced  $c_T$  formula (i.e. Eq. (16)).

(2) The calculated stress of the wrapped soil agrees well with the numerically simulated values, implying that in addition to being valid for the failure state, the stress formula for soilbags proposed by Matsuoka and Liu (2003) can also be extended to the loading/unloading state.

(3) The compressive strength of the soilbag can be predicted by the  $c_T$  formula on the basis of the maximum vertical strain, which provides a design method for the promotion and application of subgrade built with soilbags. It is also beneficial to the development of reinforced soil technologies.

This study has found that the interface friction between the loading plate and the bag material influences the compressive strength of soilbags. Further work is needed to investigate the influence of the plate–bag friction not only on the compressive strength of soilbags but also on the tension distribution in the bag and the failure mode of the soilbags (Cheng et al. 2016b), as well as the ultimate strain under vertical stress.

#### Acknowledgements

The authors greatly appreciate the support provided by the National Key R&D Program of China (Grant No. 2017YFE0128900), the Fundamental Research Funds for the Central Universities (Grant No. 2018B624X14), and the Postgraduate Research & Practice Innovation Program of Jiangsu Province (Grant No. KYCX18\_0593).

The authors also thank the reviewers for their comments and suggestions, which helped to improve the original manuscript.

#### Notation

Basic SI units are shown in parentheses.

- $\sigma$  externally applied stress (Pa)
- $\sigma_s$  stress of the soil wrapped in the bag (Pa)
- $\sigma_T$  additional stress produced by the tension of the bag (Pa)
- $\sigma_1$  major principal stress (vertical) of the soilbags (Pa)
- $\sigma_3$  minor principal stress (horizontal) of the soilbags (Pa)
- $T$  bag tensile force (N)

$B$	width of the soilbag (m)
$H$	height of the soilbag (m)
$\sigma_{1s}$	major principal stresses of the wrapped soil (Pa)
$\sigma_{3s}$	minor principal stresses of the wrapped soil (Pa)
$c_s$	cohesion of the wrapped soil (Pa)
$\varphi_s$	internal friction angle of the wrapped soil ( $^\circ$ )
$c_T$	additional cohesions of the soilbags produced by the tensile force $T$ (Pa)
$r$	radius of arc section BC (m)
$l$	length of line section AB (m)
$\varepsilon$	vertical strain of the soilbag (dimensionless)
$L_0$	total length of the bag before compression (m)
$S_0$	total area of the soilbag before compression ( $\text{m}^2$ )
$r_0$	radius of arc section BC before compression (m)
$l_0$	length of line section AB before compression (m)
$L_1$	total length of the bag after compression (m)
$S_1$	total area of the soilbag after compression ( $\text{m}^2$ )
$r_1$	radius of arc section BC after compression (m)
$l_1$	length of line section AB after compression (m)
$k$	tensile stiffness of the bag ( $\text{N}/\text{m}^2$ )
$\Delta L$	total length change of the bag (m)
$\Delta l_i$	displacement change between the two particles (m)
$V$	volume (area in two dimensions) of the measurement region ( $\text{m}^2$ )
$\mathbf{d}^c$	branch vector (m)
$\mathbf{f}^c$	branch force vector (N)
$k_n$	normal stiffness ( $\text{N}/\text{m}^2$ )
$k_s$	tangential stiffness ( $\text{N}/\text{m}^2$ )
$pb-k_n$	normal stiffness of the parallel bond ( $\text{N}/\text{m}^2$ )

$pb-k_s$	shear stiffness of the parallel bond (N/m <sup>2</sup> )
$\beta$	ratio of the damping constant to the critical damping constant (dimensionless)
$\mu$	friction coefficient of the particles (dimensionless)
$\rho$	density of the particles (kg/m <sup>3</sup> )
$\sigma_{xx}$	stress of the wrapped soil in x direction (Pa)
$\sigma_{yy}$	stress of the wrapped soil in y direction (Pa)

### Abbreviations

DEM discrete element method

### References

- Ansari, Y., Merifield, R., Yamamoto, H. & Sheng, D.C. (2011). Numerical analysis of soilbags under compression and cyclic shear. *Computers and Geotechnics*, **38**, No. 5, 659-668.
- Bai, F. Q., Liu, S.H. & Wang, Y. Q. (2010). Research on reinforcement mechanism and failure strength of soilbags. *Rock and Soil Mechanics*, **31**, 172-176 (in Chinese).
- Ball, K. (1991). Volume ratios and a reverse isoperimetric inequality. *Journal of the London Mathematical Society*, **s2**, 44.
- Cheng, H.Y., Luding, S., Saitoh, K. & Magnanimo, V. (2020). Elastic wave propagation in dry granular media: effects of probing characteristics and stress history. *International Journal of Solids and Structures*, **187**, 85-99.
- Cheng, H.Y. & Yamamoto, H. (2015). Modeling microscopic behavior of geotextile-wrapped soil by discrete element method. *Japanese Geotechnical Society Special Publication*, **2** No. 65, 2215-2220.
- Cheng, H.Y. & Yamamoto, H. (2016a). Evaluating the Performance of Geotextile Wrapped/Layered Soil: A Comparative Study Using the DEM. In *4th GeoChina International Conference 2016: Sustainable Civil Infrastructures: Innovative Technologies for Severe Weathers and Climate Changes* (pp. 122-130). American Society of Civil Engineers.
- Cheng, H.Y., Yamamoto, H. & Thoeni, K. (2016b). Numerical study on stress states and fabric anisotropies in soilbags using the DEM. *Computers and Geotechnics*, **76**, 170-183.

- Cheng, H.Y., Yamamoto, H., Thoeni, K. & Wu, Y. (2017). An analytical solution for geotextile-wrapped soil based on insights from DEM analysis. *Geotextiles and Geomembranes*, **45**, No. 4, 361-376.
- Cundall, P.A. (1971). A computer model for simulating progressive, large scale movements in blocky rock systems. *Proceedings of the International Symposium on Rock Fractures*. Nancy, France II-8, pp. 1-12.
- Cundall, P.A. & Strack, O.D.L. (1979). A discrete numerical model for granular assemblies. *Geotechnique*, **29**, No. 1, 47-65.
- Ding, G.Y., Wu, J.L., Wang, J., Fu, H.T. & Liu, F.Y. (2018). Experimental study on vibration reduction by using soilbag cushions under traffic loads. *Geosynthetics International*, **25**, No. 3, 322-333.
- Fan, K.W., Liu, S.H., Cheng, Y.P. & Wang, Y. (2019). Sliding stability analysis of a retaining wall constructed by soilbags. *Géotechnique Letters*, **9**, 1-7.
- Lee, Y.J. & Song, K.J. (2010). Shearing characteristics of aluminium rods using plane strain-shear box test and close range photogrammetric technique. *Journal of the Korean Geotechnical Society*, **26**, No. 8, 5-14 (in Korean).
- Li, Z., Liu, S.H., Wang, L.J. & Zhang, C.C. (2013). Experimental study on the effect of frost heave prevention using soilbags. *Cold Regions Science and Technology*, **85**, 109-116.
- Liu, H.B. (2016). Required reinforcement stiffness for vertical geosynthetic-reinforced-soil walls at strength limit state. *Géotechnique*, **66**, No. 5, 424-434.
- Liu, H.B., Yang, G.Q., Wang, H. & Xiong, B.L. (2017). A large-scale test of reinforced soil railway embankment with soilbag facing under dynamic loading. *Geomechanics and Engineering*, **12**, No. 4, 579-593.
- Liu, S.H. (2017). *The principle and application of soilbags*. Science Press, Beijing (in Chinese).
- Liu, S.H., Fan, K.W. & Xu, S.Y. (2019). Field study of a retaining wall constructed with clay-filled soilbags. *Geotextiles and Geomembranes*, **47**, No. 1, 87-94.
- Liu, S.H., Gao, J.J., Wang, Y.Q. & Weng, L.P. (2014). Experimental study on vibration reduction by using soilbags. *Geotextiles and Geomembranes*, **42**, No. 1, 52-62.
- Liu, S.H., Jia, F., Shen, C.M. & Weng, L.P. (2018). Strength characteristics of soilbags under inclined loads. *Geotextiles and Geomembranes*, **46**, No. 1, 1-10.

- Liu, S.H., Jia, F., Chen, X.L. & Li, L.J. (2020). Experimental study on seismic response of soilbags-built retaining wall. *Geotextiles and Geomembranes* (<https://doi.org/10.1016/j.geotexmem.2020.03.006>).
- Liu, S.H., Lu, Y., Weng, L.P. & Bai, F.Q. (2015). Field study of treatment for expansive soil/rock channel slope with soilbags. *Geotextiles and Geomembranes*, **43**, No. 4, 283-292.
- Liu, S.H. & Matsuoka, H. (2003). Microscopic interpretation on a stress-dilatancy relationship of granular materials. *Soils and Foundation*, **43**, No. 3, 73-84.
- Liu, S.H. & Matsuoka, H. (2007). A new earth reinforcement method by soilbags. *Rock and Soil Mechanics*, **28**, No. 8, 1665-1670 (in Chinese).
- Lu, M. & McDowell, G.R. (2010). Discrete element modelling of railway ballast under monotonic and cyclic triaxial loading. *Géotechnique*, **60**, No. 6, 459.
- Matsuoka, H. & Liu, S.H. (1999). Bearing capacity improvement by wrapping a part of foundation. *Japan Society of Civil Engineers (JSCE)*, No. 617/III-46, 235-249 (in Japanese).
- Matsuoka, H. & Liu, S.H. (2003). New earth reinforcement method by soilbags (“Donow”). *Soils and Foundations*, **43**, No. 6, 173-188.
- Matsuoka, H. & Liu, S.H. (2006). *A New Earth Reinforcement Method Using Soilbags*. Taylor & Francis/Balkema, the Netherlands.
- Matsuoka, H., Chen, Y., Kodama, H., Yamaji, Y. & Tanaka, R. (2000). Mechanical properties of soilbags and unconfined compression tests on model and real soilbags. *Proceeding of the 35th Japan National Conference on Geotechnical Engineering*, Gifu, Japan, **544**, 1075-1076 (in Japanese).
- Pham, H.V., Dias, D. & Dudchenko, A. (2020). 3D modeling of geosynthetic-reinforced pile-supported embankment under cyclic loading. *Geosynthetics International*, **27**, No. 2, 157-169.
- Shen, C.M., Liu, S.H., Wang, L.J. & Wang, Y.S. (2019). Micromechanical modeling of particle breakage of granular materials in the framework of thermomechanics. *Acta Geotechnica*, **14**, No. 4, 939-954.
- Sheng, T., Bian, X. C., Liu, G.B., Xiao, C., Chen, Y. & Li, Y. (2020). Experimental study on the sandbag isolator of buildings for subway-induced vertical vibration and secondary

air-borne noise. *Geotextiles and Geomembranes*

(<https://doi.org/10.1016/j.geotextmem.2020.02.008>).

- Tantono, S.F. & Bauer, E. (2008a). Influence of interface friction on the bearing capacity of a sandbag element. *Proceedings of 11th Baltic Sea Geotechnical Conference, Geotechnics in Maritime Engineering*, Gdansk, Poland, 779-784.
- Tantono, S.F. & Bauer, E. (2008b). Numerical simulation of a soilbag under vertical compression. *Proceedings of the 12th International Conference of International Association for Computer Methods and Advances in Geomechanics (IACMAG)*, Goa, India, 433-439.
- Wang, L.J., Liu, S.H. & Zhou, B. (2015). Experimental study on the inclusion of soilbags in retaining walls constructed in expansive soils. *Geotextiles and Geomembranes*, **43**, No. 1, 89-96.
- Wang, L.J., Liu, S.H., Liao, J. & Fan, K.W. (2019a). Field load tests and modelling of soft foundation reinforced by soilbags. *Geosynthetics International*, **26**, No. 6, 580-591.
- Wang, Y.Q., Li, X., Liu, K. & Liu, G. (2019b). Experiments and DEM analysis on vibration reduction of soilbags. *Geosynthetics International*, **26**, No. 5, 551-562.
- Wang, Y.Q., Liu, K., Li, X., Ren, Q.B., Li, L.L., Zhang, Z.H. & Li, M.C. (2019c). Experimental and upper-bound study of the influence of soilbag tail length on the reinforcement effect in soil slopes. *Geotextiles and Geomembranes*, **47**, No. 5, 610-617.
- Yamamoto, S. (1995). Fundamental study on mechanical behavior of granular materials by DEM. Dr. Eng. Thesis, Nagoya Institute of Technology, Japan (in Japanese).
- Ye, B., Muramatsu, D., Ye, G.L. & Zhang, F. (2011). Numerical assessment of vibration damping effect of soilbags. *Geosynthetics International*, **18**, No. 4, 159-168.
- Zhao, C.F., Yin, Z.Y., Misra, A. & Hicher, P.Y. (2018). Thermomechanical formulation for micromechanical elasto-plasticity in granular materials. *International Journal of Solids and Structures*, **138**, 64-75.

Table 1. Input parameters used in DEM simulation

	Soil Particle	Bag particle	Wall
$k_n$ (N/m <sup>2</sup> )	$1.0 \times 10^9$	$1.0 \times 10^7$	$1.0 \times 10^9$
$k_s$ (N/m <sup>2</sup> )	$1.0 \times 10^8$	0	$1 \times 10^8$
$pb-k_n$ (N/m <sup>2</sup> )	-	$1.0 \times 10^8$	-
$pb-k_s$ (N/m <sup>2</sup> )	-	$1.0 \times 10^7$	-
$\beta$	0.2	-	-
$\mu$	0.2	0	0
$\rho$ (kg/m <sup>3</sup> )	2650	440	-

### Figure captions

Fig. 1. Stresses acting on two-dimensional model soilbag and on particles inside the soilbag:

(a) Stresses acting on soilbag; (b) Stresses acting on particles inside soilbag

Fig. 2. Sketch of the compression process of the soilbag

Fig. 3. DEM model of one soilbag under vertical load

Fig. 4. Loading process of the cyclic compression test

Fig. 5. Inter-particle contact forces of a soilbag under cyclic loading (unit: N): (a) loading

$\sigma=10$  kPa; (b) loading  $\sigma=60$  kPa; (c) unloading  $\sigma=10$  kPa

Fig. 6. Vector distribution of displacement in a soilbag under cyclic loading (unit: m): (a)

loading  $\sigma=10$  kPa; (b) loading  $\sigma=60$  kPa; (c) unloading  $\sigma=10$  kPa

Fig. 7. Predicted and simulated tensile behaviour of the bag against vertical strain

Fig. 8. Evolution of stress state of soil wrapped in a soilbag during cyclic shear test: (a)  $\sigma_{yy}$  ;

(b)  $\sigma_{xx}$

Fig. 9. Simulation of compression behaviour of soilbags under vertical cyclic loading

Fig. 10. Cyclic uniaxial compression test of soilbags with aluminium rods as the soil

Fig. 11. Experimental result of compression behaviour of soilbags under vertical cyclic

loading

Fig. 12. Simulation of compression behaviour of soilbags under vertical cyclic loading by

frictional rigid walls

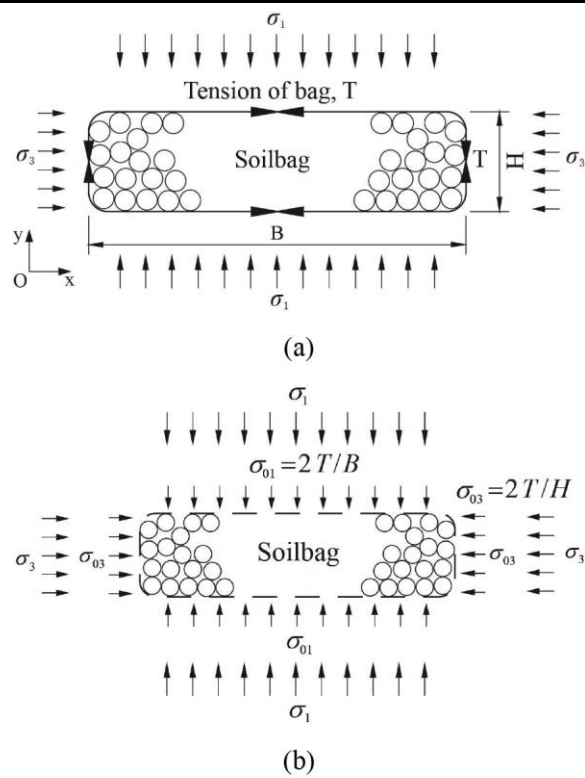


Fig. 1

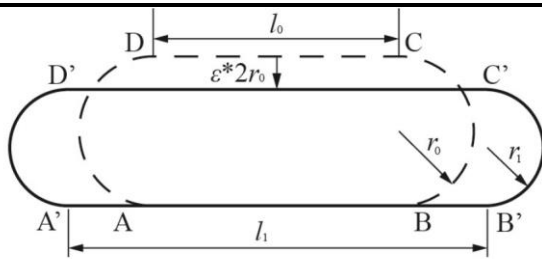


Fig. 2

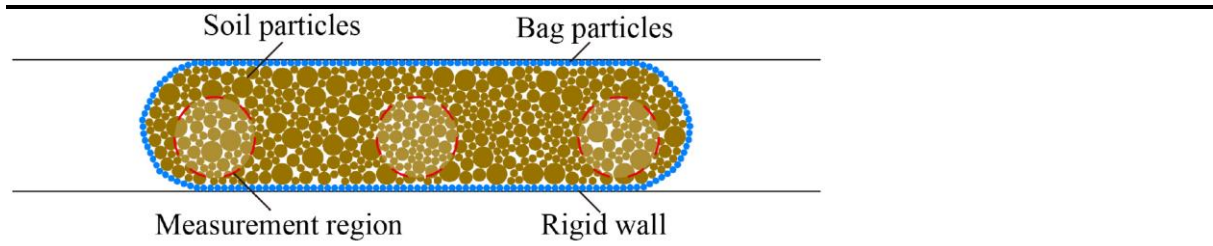


Fig. 3

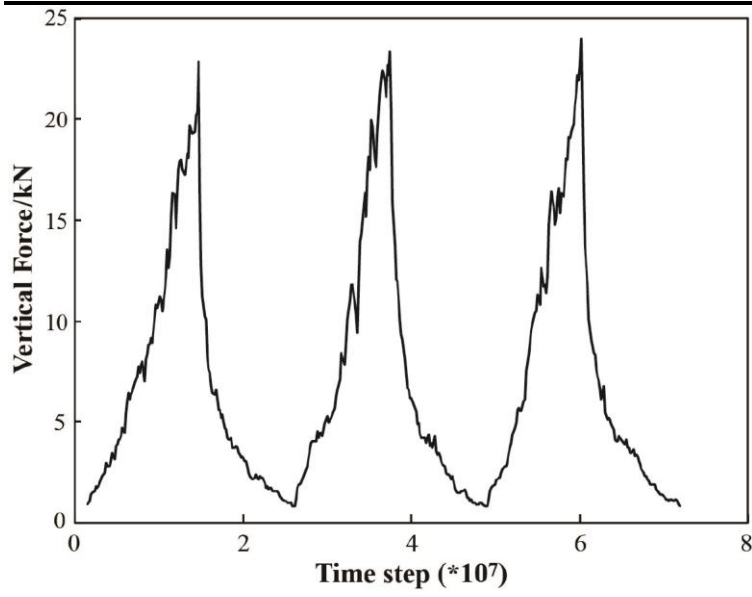


Fig. 4

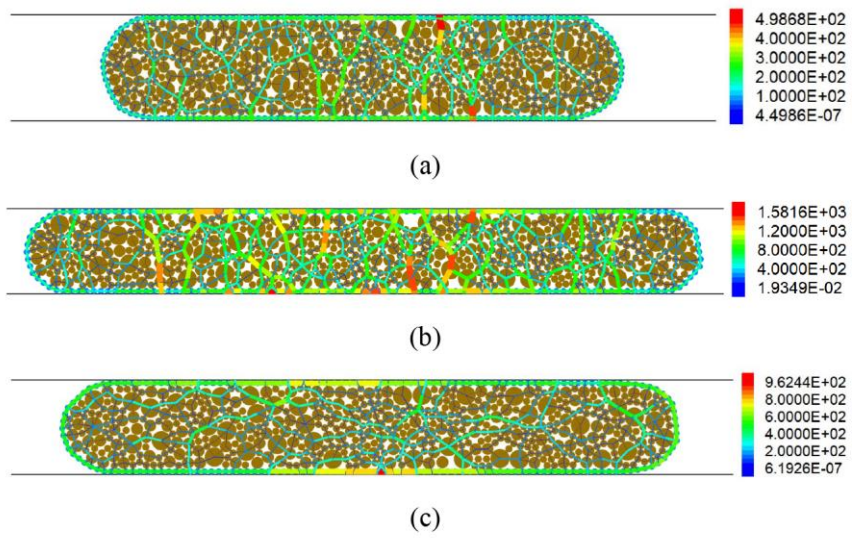


Fig. 5

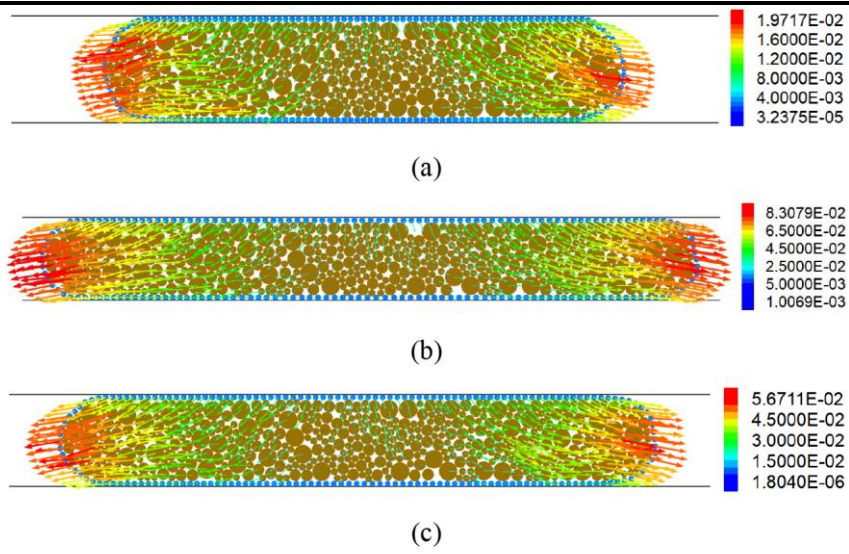


Fig. 6

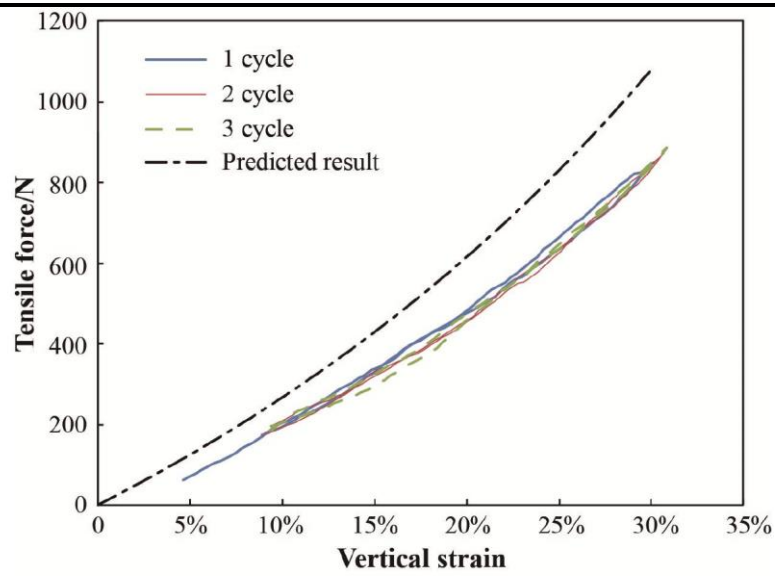
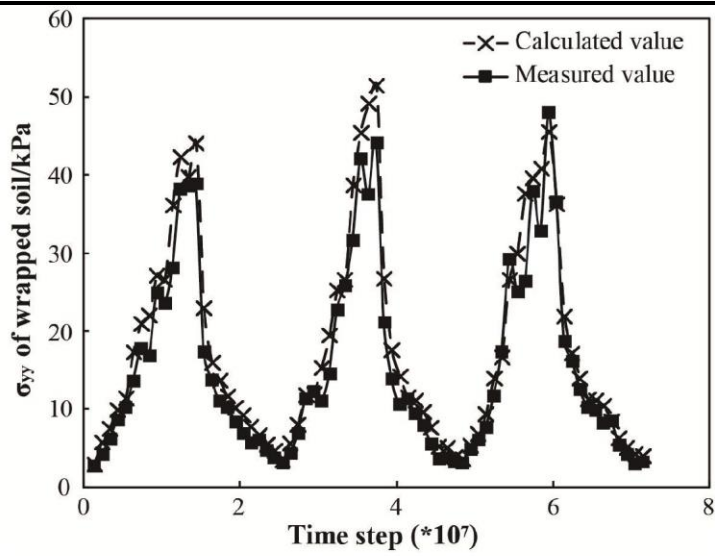
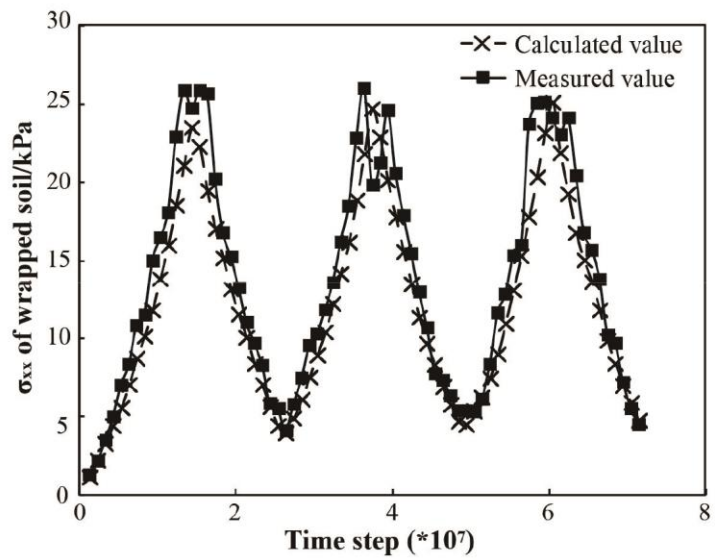


Fig. 7



(a)



(b)

Fig. 8

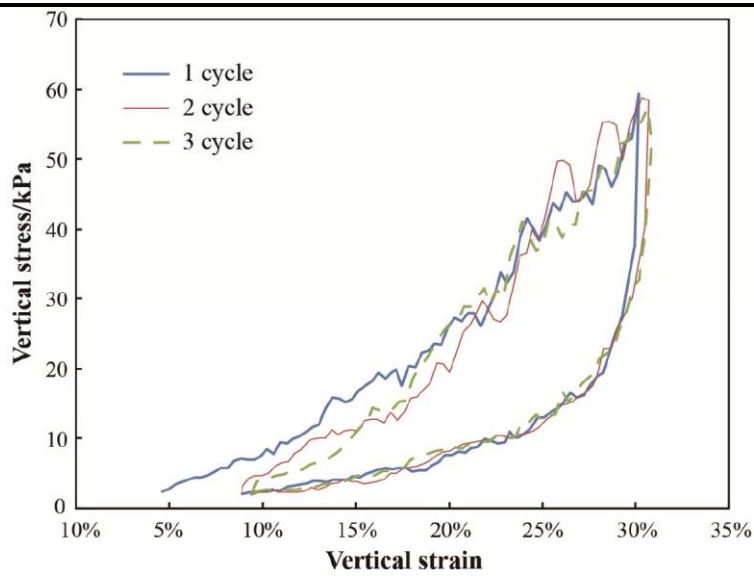


Fig. 9

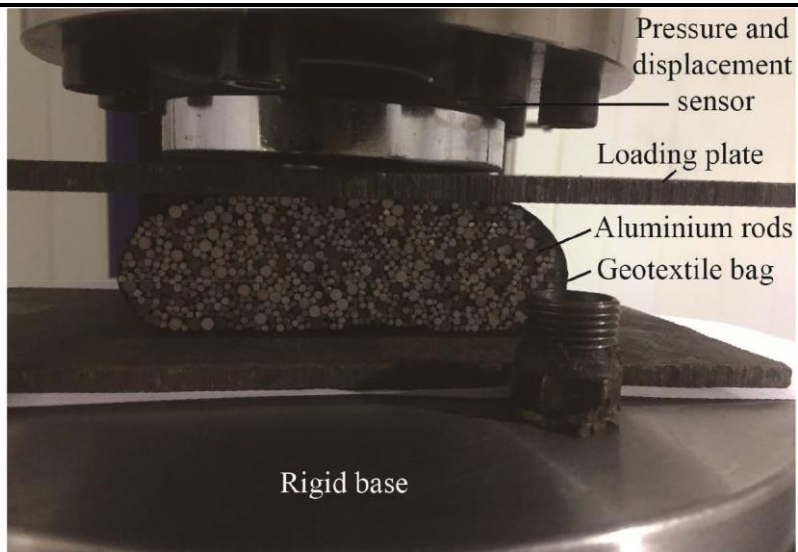


Fig. 10

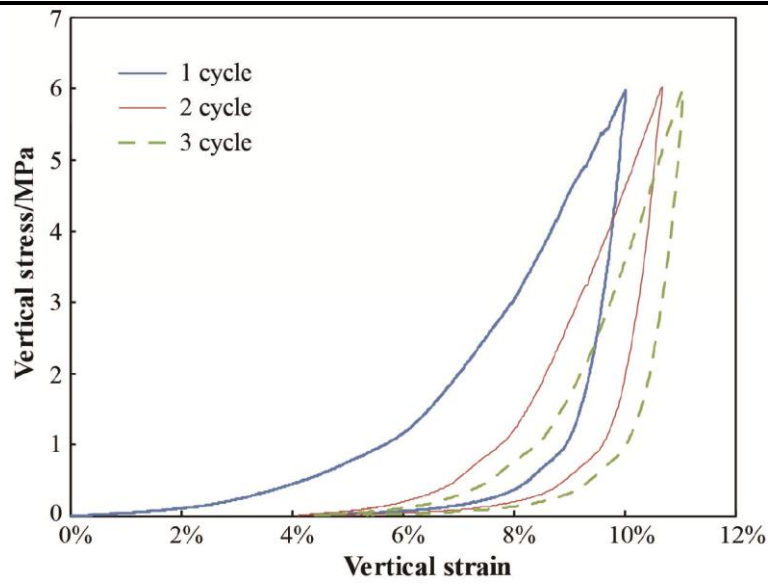


Fig. 11

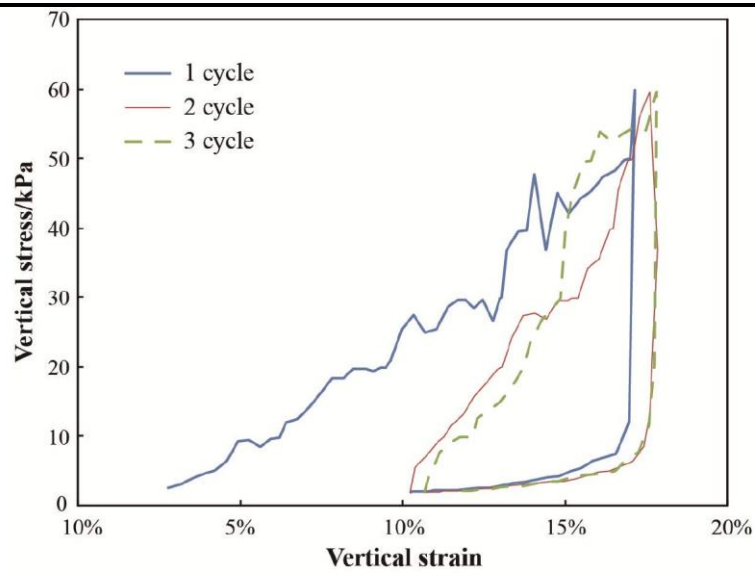


Fig. 12